



UNIVERSITY OF  
**ALBERTA**

## **ULF Waves - Drift and Drift-Bounce Resonance**

**R. Rankin<sup>1</sup>, C. Wang<sup>1</sup>, Y. Wang<sup>2</sup>, Q.-G. Zong<sup>2</sup>,**

**K. Takahashi<sup>3</sup>, A. W. Degeling<sup>4</sup>,**

**<sup>1</sup>University of Alberta, Edmonton, Canada.**

**<sup>2</sup>Peking University, Beijing, China.**

**<sup>3</sup>The Johns Hopkins Applied Physics Laboratory, USA.**

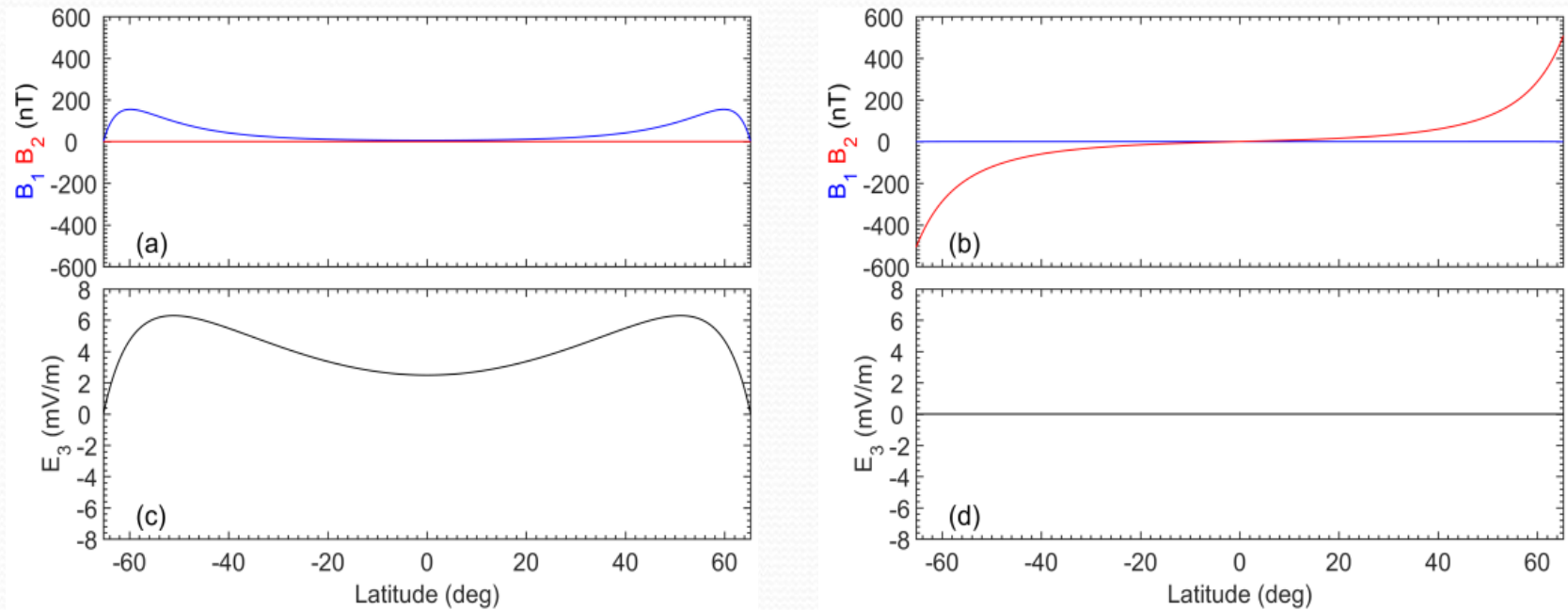
**<sup>4</sup>Shandong University, Weihai, China.**



# Outline

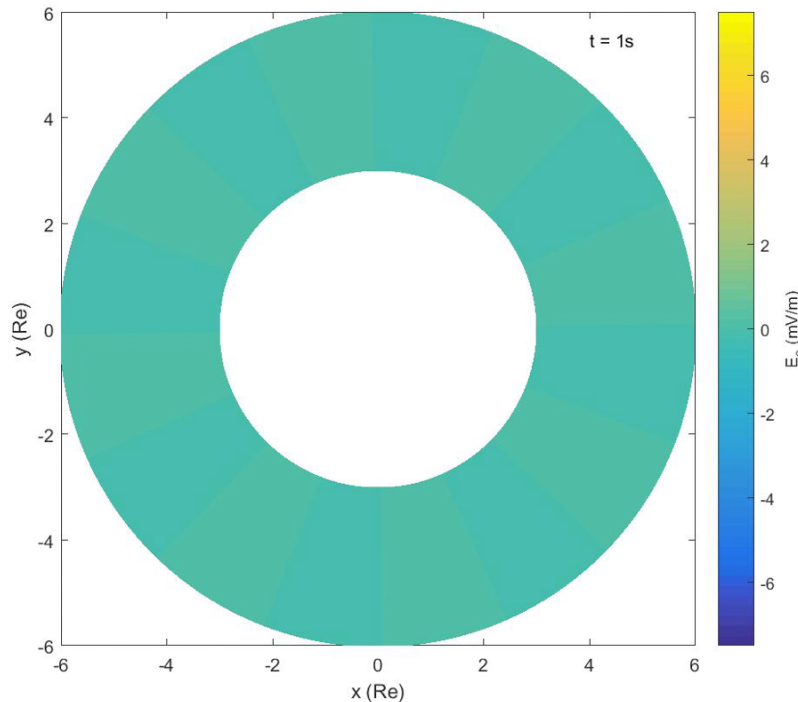
- Simplified model of driven ULF Waves in a dipole field.
- Single particle examples of drift resonance and drift-bounce resonance.
- Electron drift resonance – guiding center simulation of electron dynamics following an interplanetary shock [Claudepierre et al., GRL, 2013]; [Pancake-shaped PSD](#).
- Ion drift resonance – full Lorentz force simulation of ion dynamics resulting from particle-driven ULF waves [Takahashi et al., JGR, 2018]; [Butterfly-shaped PSD](#).
- A possible explanation for the absence of ion differential flux at  $90^\circ$  pitch angle in the Takahashi event.

# ULF Poloidal Wave at L=5.7



**E** and **B** components for  $f=10\text{mHz}$  and  $m=35$ . Left column shows the **compressional magnetic field**  $B_1$  and **azimuthal electric field**  $E_3$  (both in phase). Right column shows wave fields a  $\frac{1}{4}$  period later.

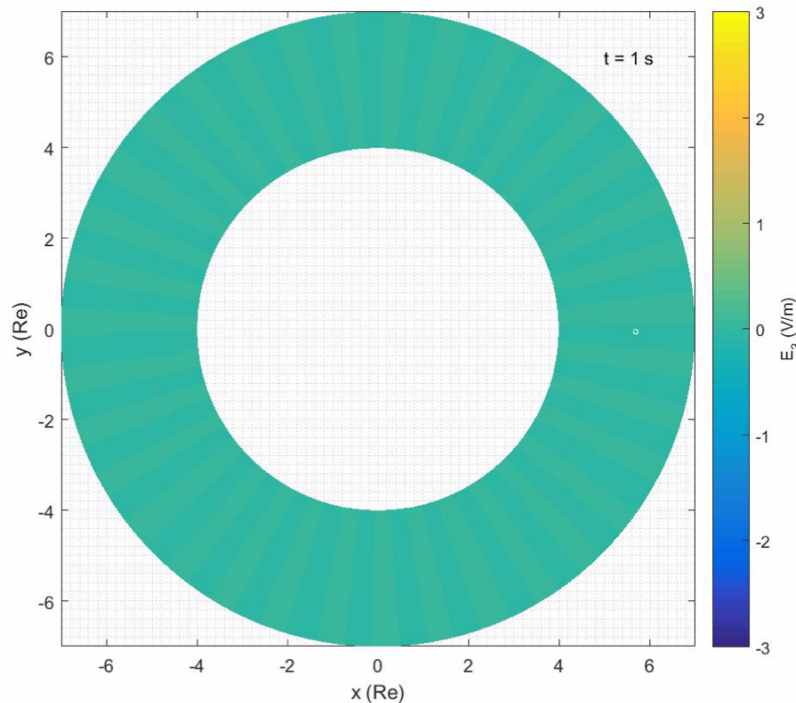
# Model for Driven ULF Waves\*



- **Equatorial view** of poloidal electric field excited by monochromatic constant amplitude driver wave.
- Azimuthal wavenumber  $m=8$ .
- Tilted wave pattern relative to background field.
- Phase mixing in radial direction.
- $180^\circ$  phase change in L.

\*JGR paper in which the wave model is described is under review.

# Drift Resonance and H<sup>+</sup>

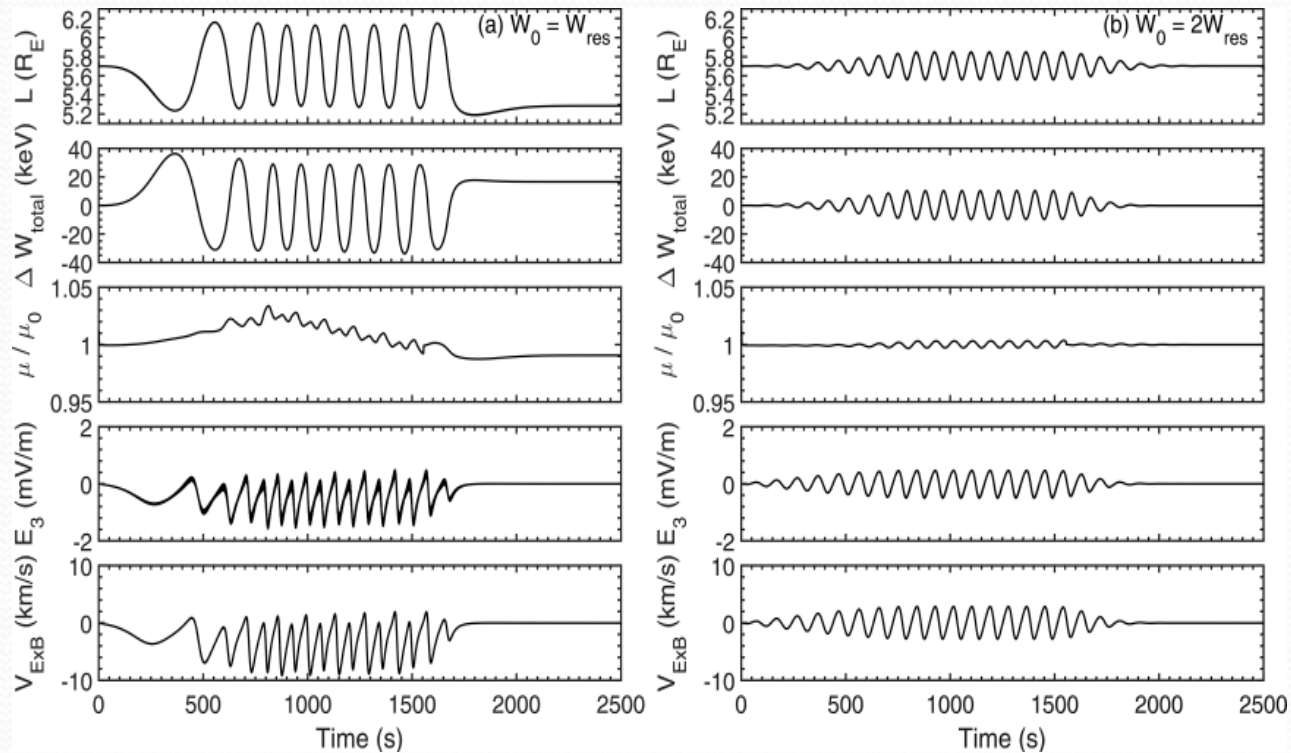


- Equatorial view of poloidal electric field excited by a monochromatic constant amplitude driver.
- Ion is trapped in a range of  $L$  and surfs a wave front that is tilted relative to the background dipole field.
- Poincare plots show closed trajectories consistent with a drift resonant interaction with ULF waves:

**Note that the wave amplitude grows and then decays over several wave periods.**

$$\omega - m\omega_d = 0$$

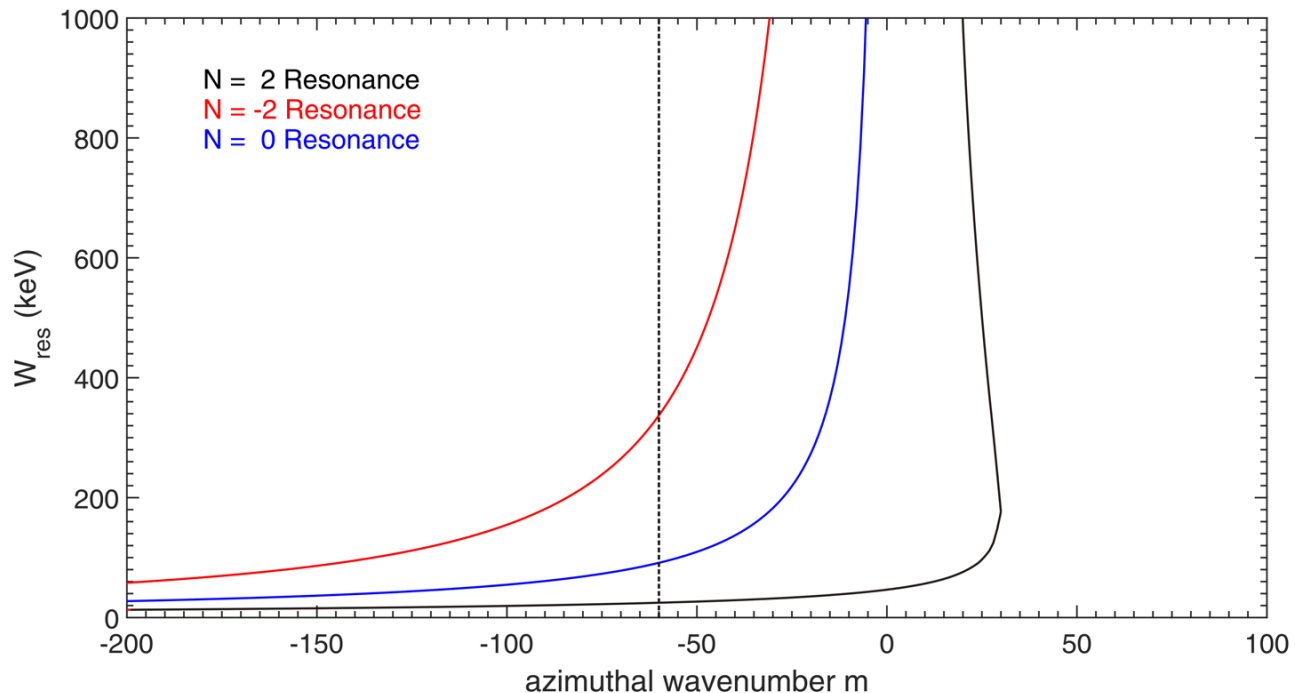
# Resonant vs Non-Resonant H<sup>+</sup>



- Trajectory parameters for resonant and non-resonant H<sup>+</sup>.
- **Left Column:** initial energy close to resonance energy  $\sim 150$  keV.  
**Right Column:** initial energy  $\sim 300$  keV.
- Changes in  $L$ , energy, and  $\mu$  are larger for resonant ions.

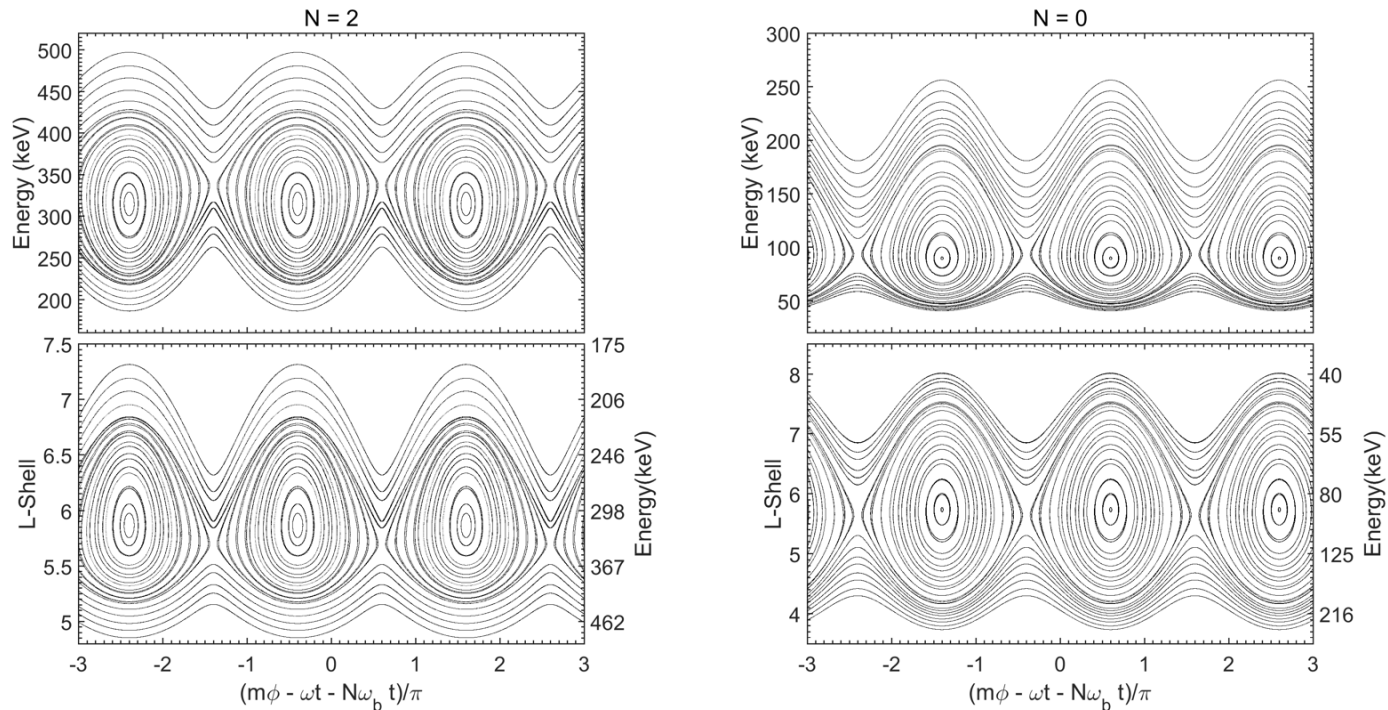
# Drift-Bounce Resonance

$$\omega - m\omega_d = N\omega_b$$



Resonance energy of  $O^+$  as a function of azimuthal wavenumber  $m$  and different  $N$  in a dipole field at  $L = 5.7$ . Wave with  $m > 0$  propagates eastward. For  $N > 0$ , drift-bounce resonance occurs for ions moving eastward in the wave frame. Here,  $f = 10$  mHz and ions have an equatorial PA of  $30^\circ$ .

# Drift-Bounce Resonance

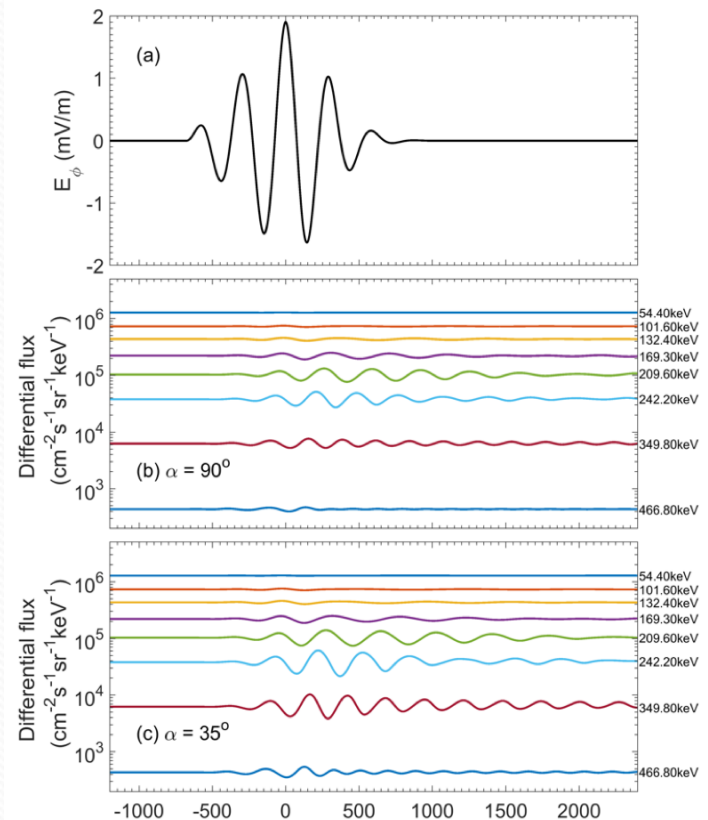
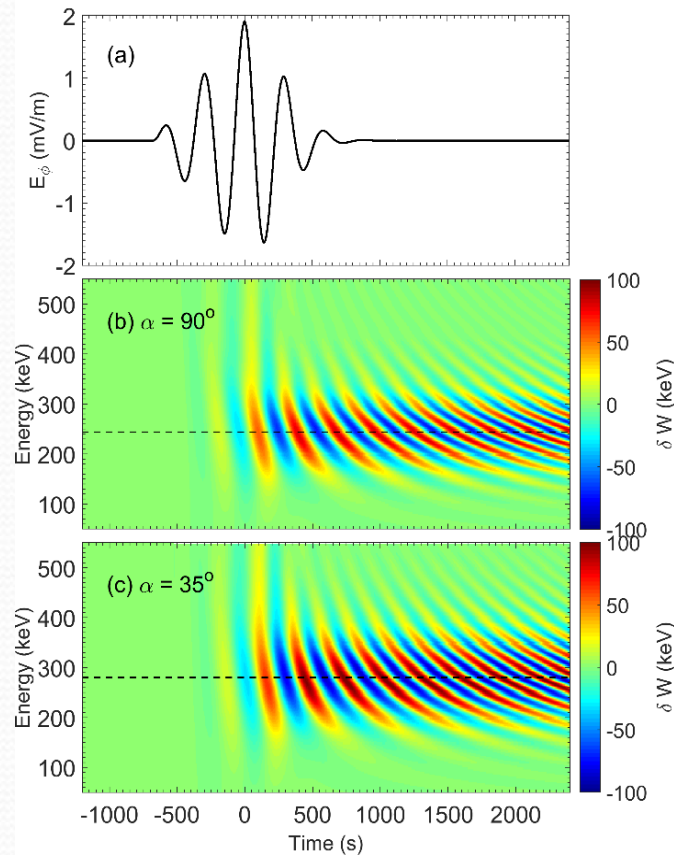


Poincaré maps showing trapping of test particle ions with initially constant first and second adiabatic invariant. The wave amplitude is fixed at  $23\text{mVm}^{-1}$ .

$$\omega - m\omega_d = N\omega_b$$

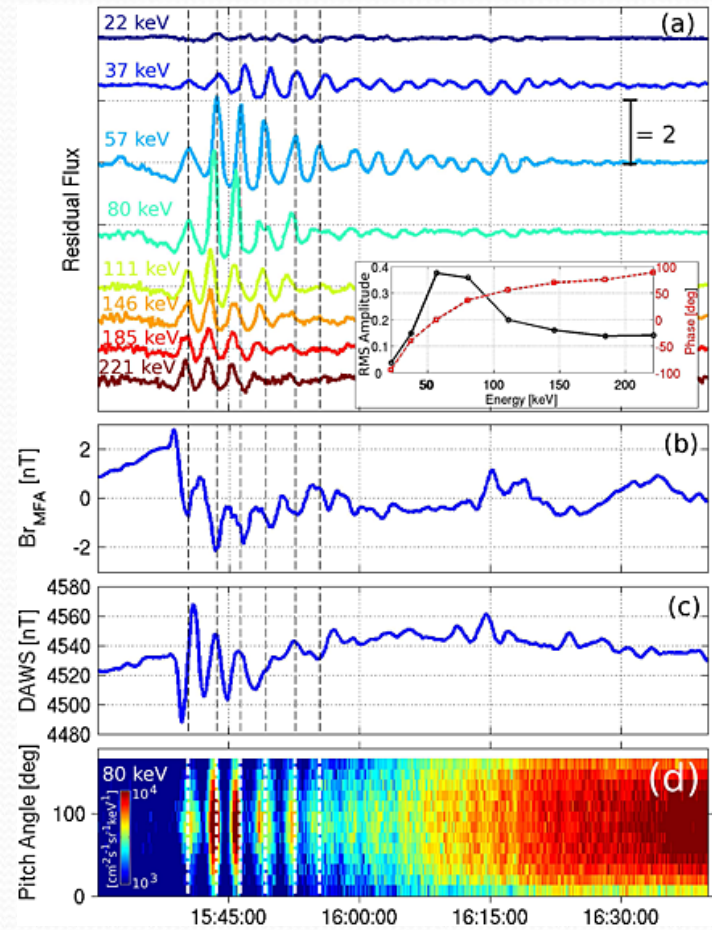
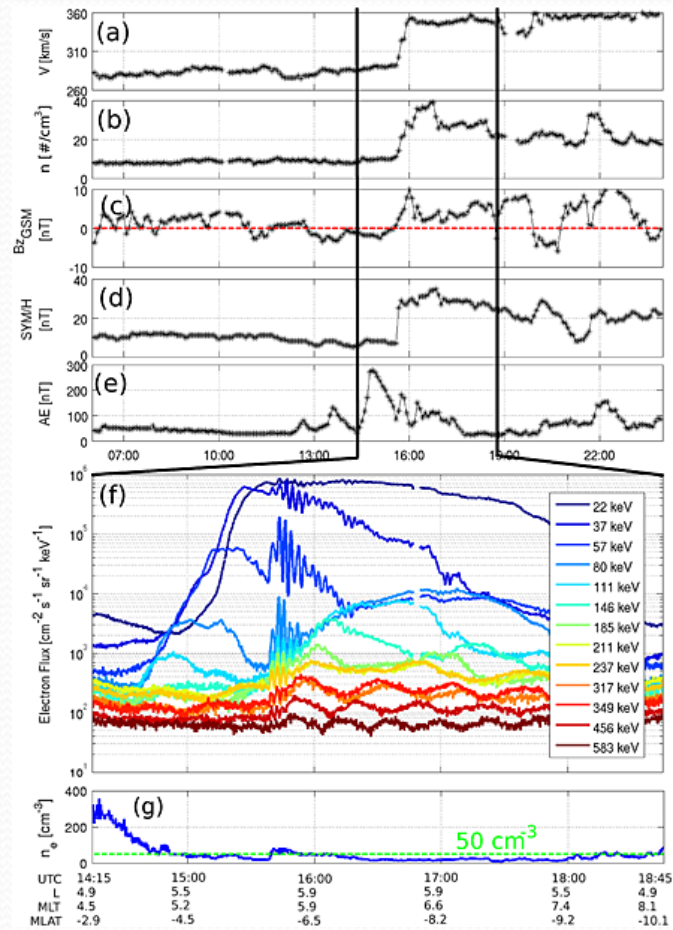


# PSD From Backward Tracing



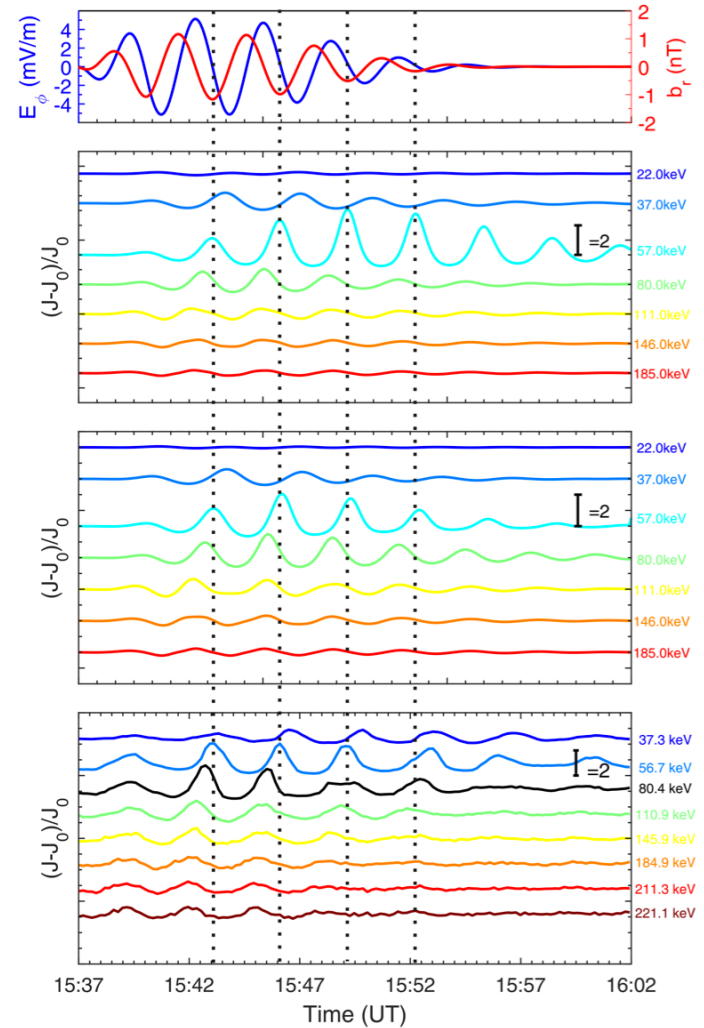
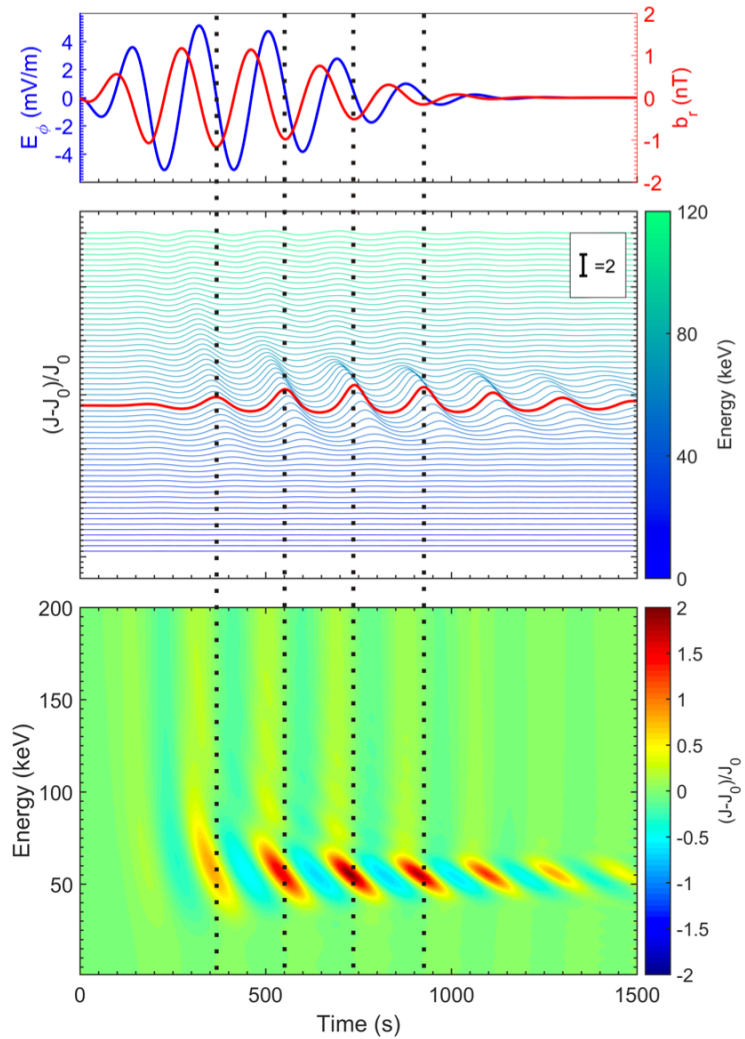
Backward-tracing can be used to determine energy changes of  $\text{H}^+$  with PA's of  $90^\circ$  and  $35^\circ$ ; left panels (b) and (c), respectively. Panels (b) and (c) on the right show binned differential flux (using data from left column).

# Claudepierre Event 2013

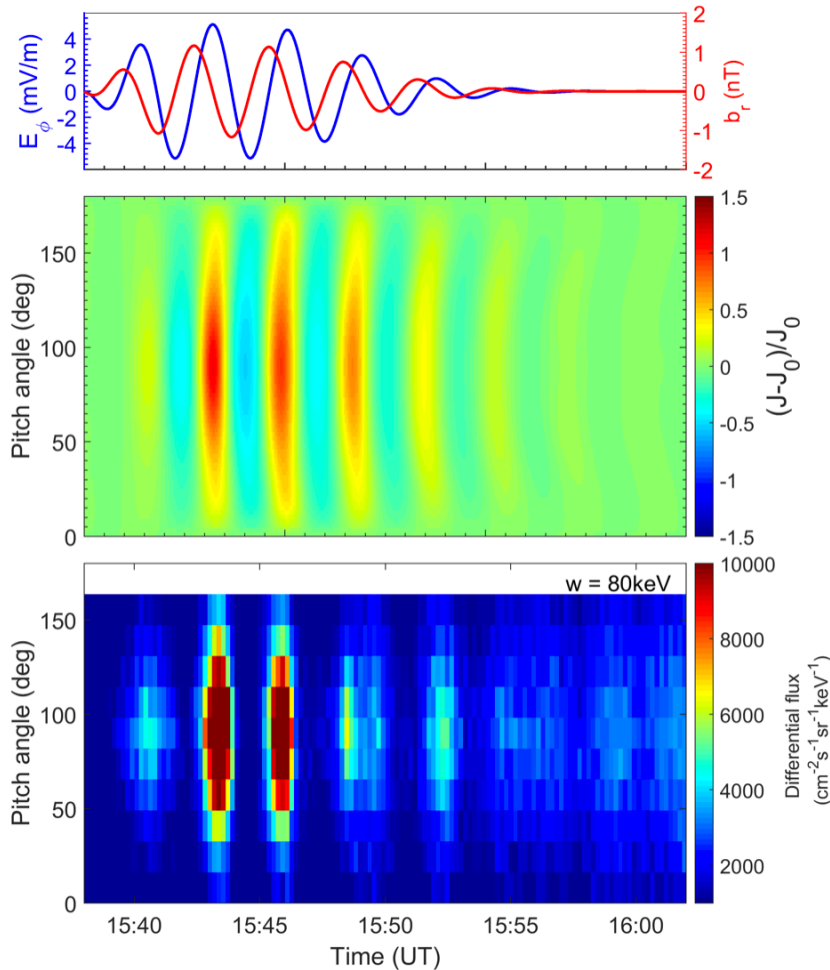


VAPs observations of drift-resonant ULF waves and 20–500keV electrons on 31<sup>st</sup> Oct. 2012. Fundamental poloidal mode excited following IP shock

# Model-Data Comparison

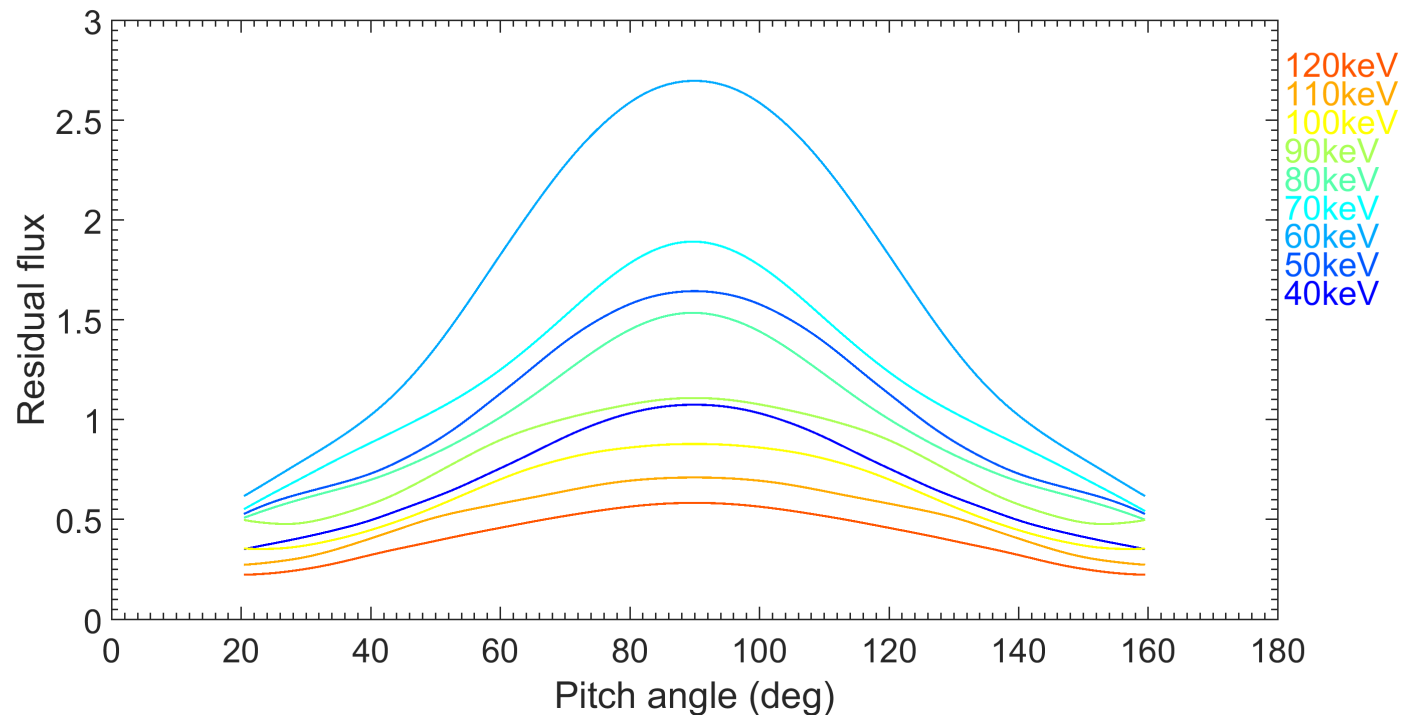


# Model-Data Comparison



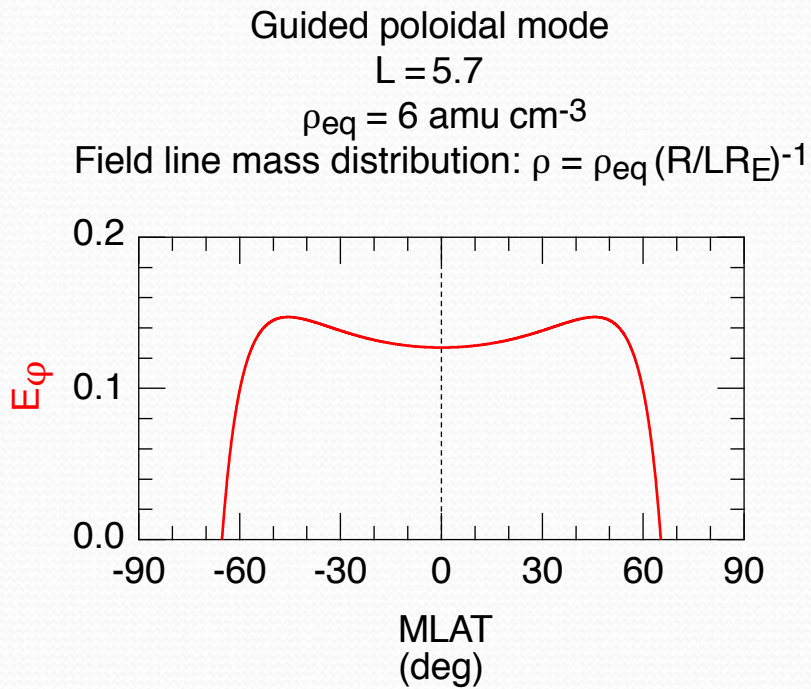
- Top panel: Wave amplitude profile used in simulations.
- Middle panel: Simulated residual flux as a function of pitch angle and time.
- Bottom panel adapted from Claudepierre et al. [2013] shows the differential flux from the 80keV energy channel on MagEIS-A.

# Model-Data Comparison

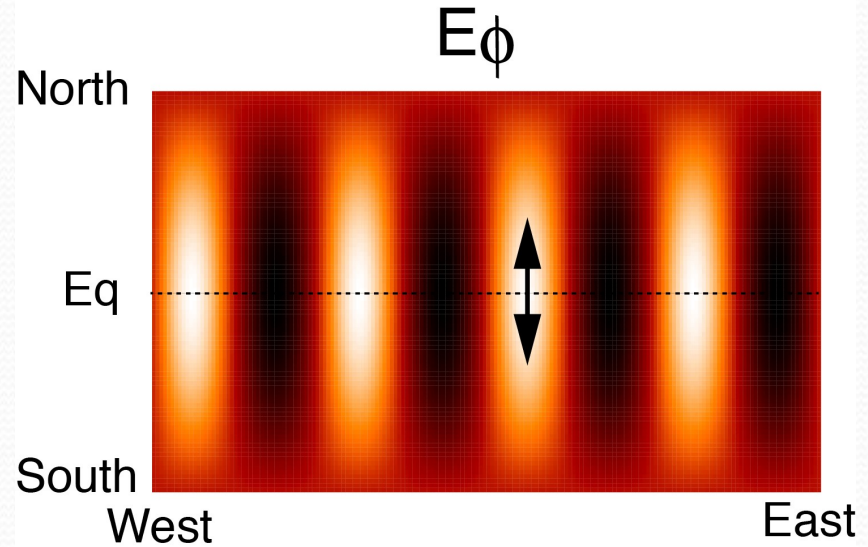


VAPs observations of electron drift resonance on 31<sup>st</sup> Oct. 2012. Fundamental poloidal mode excited following an IP shock. The electrons form a pancake distribution (cf. ions discussed next).

# Giant Pulsations



Takahashi Fall AGU 2016



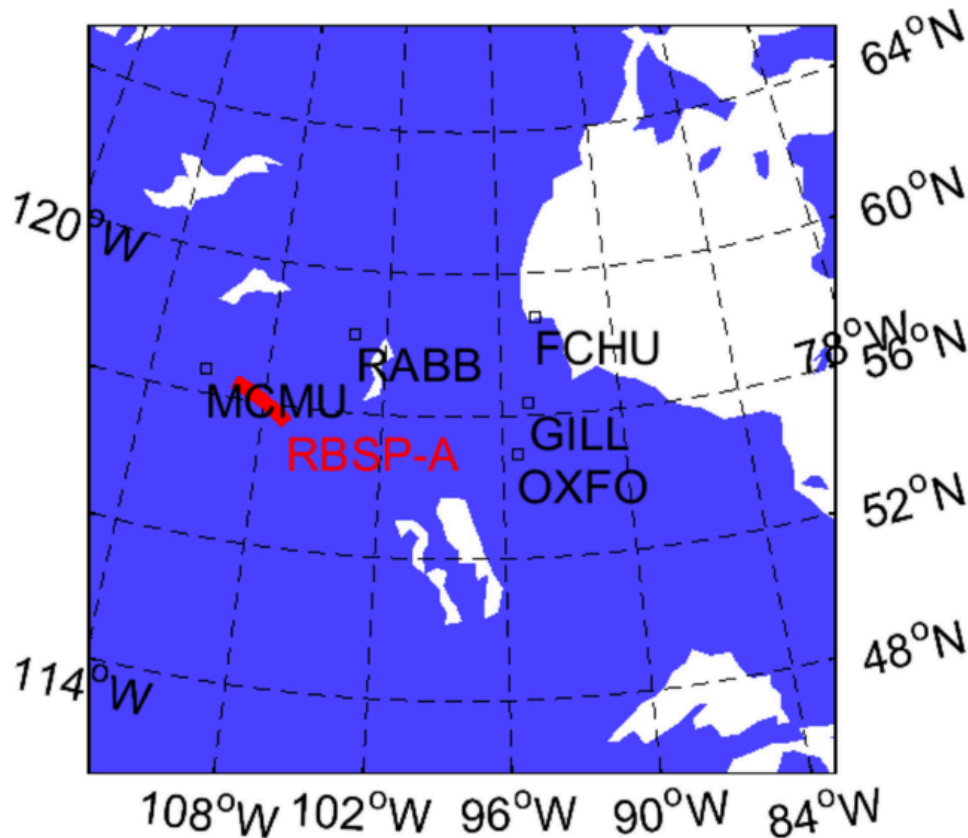
$$\omega - m\omega_d = 0$$

At  $L=5.7$ , the **drift-resonance condition is satisfied for  $\sim 150 \text{ keV H}^+$  ions** interacting with a ULF wave with  $f \sim 10 \text{ mHz}$  propagating **westward with  $m \sim 35$** .

# Giant Pulsations

- On October 6<sup>th</sup>, 2012, Giant Pulsations (Pgs) propagating westward in the morning sector were observed [Takahashi et al., 2016 AGU Fall Meeting].
- The Pgs were detected by RBSP-A and ground-based magnetometers in the CARISMA magnetometer array.
- Ion flux modulations were observed by the MagEIS instrument on RBSP-A, with 35° pitch-angle modulation amplitudes much larger than at 90°.
- Fundamental mode  $m \sim 35$  drift resonance with H<sup>+</sup> ions.
- ULF wave and test particle modeling is presented that reproduce the observations.

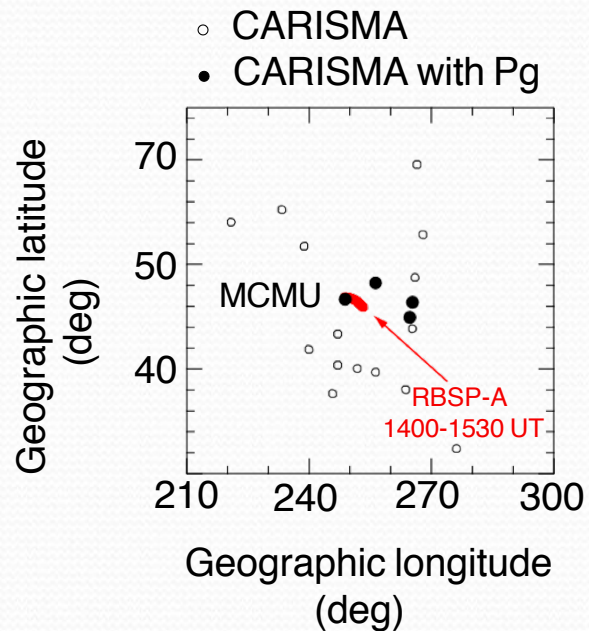
# CARISMA and RBSP-A Conjunction



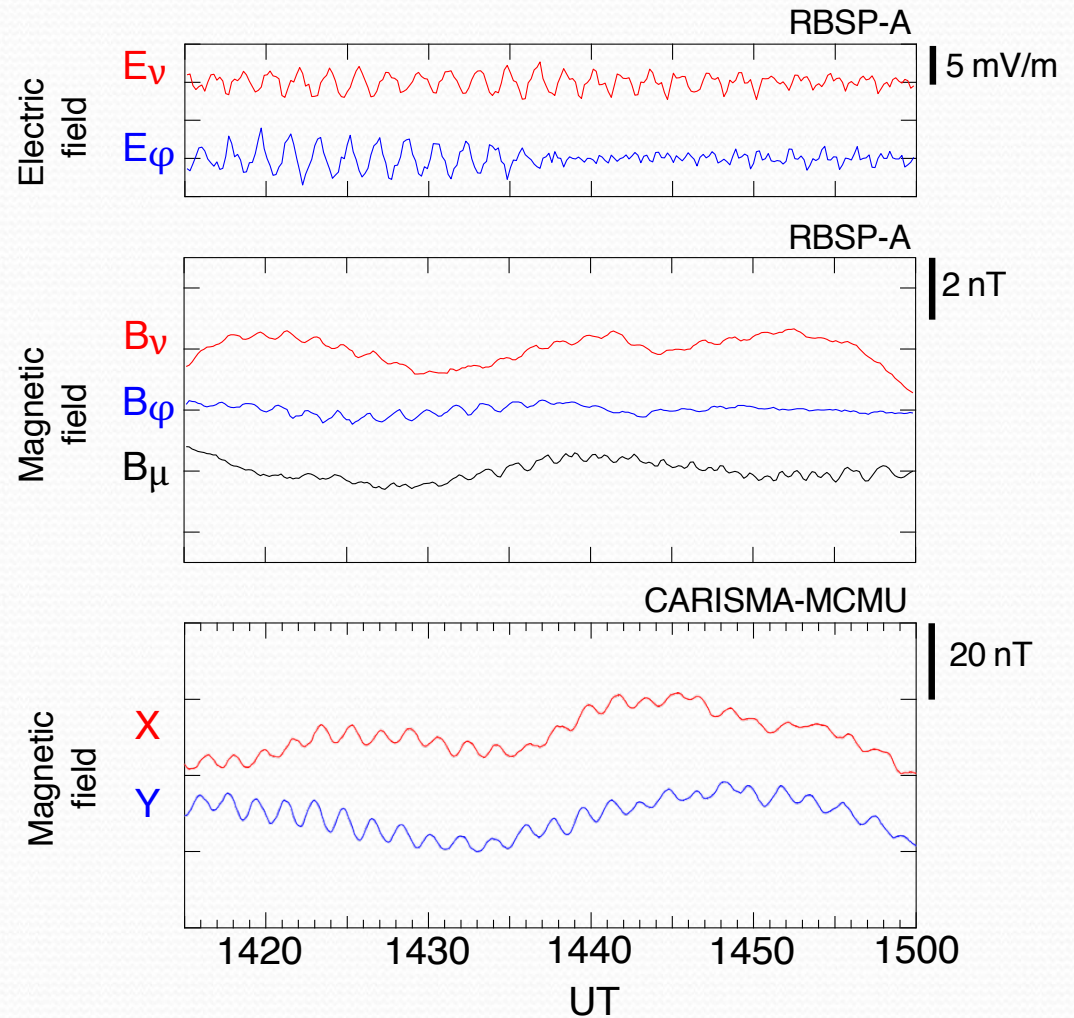
- Magnetometer stations in the CARISMA array.
- Ground track of RBSP-A intersects the MCMU station.
- MCMU and GILL observations are similar but signals at RABB and OXFO are weaker.
- Wave is highly localized in latitude.



# RBSP-A Observations

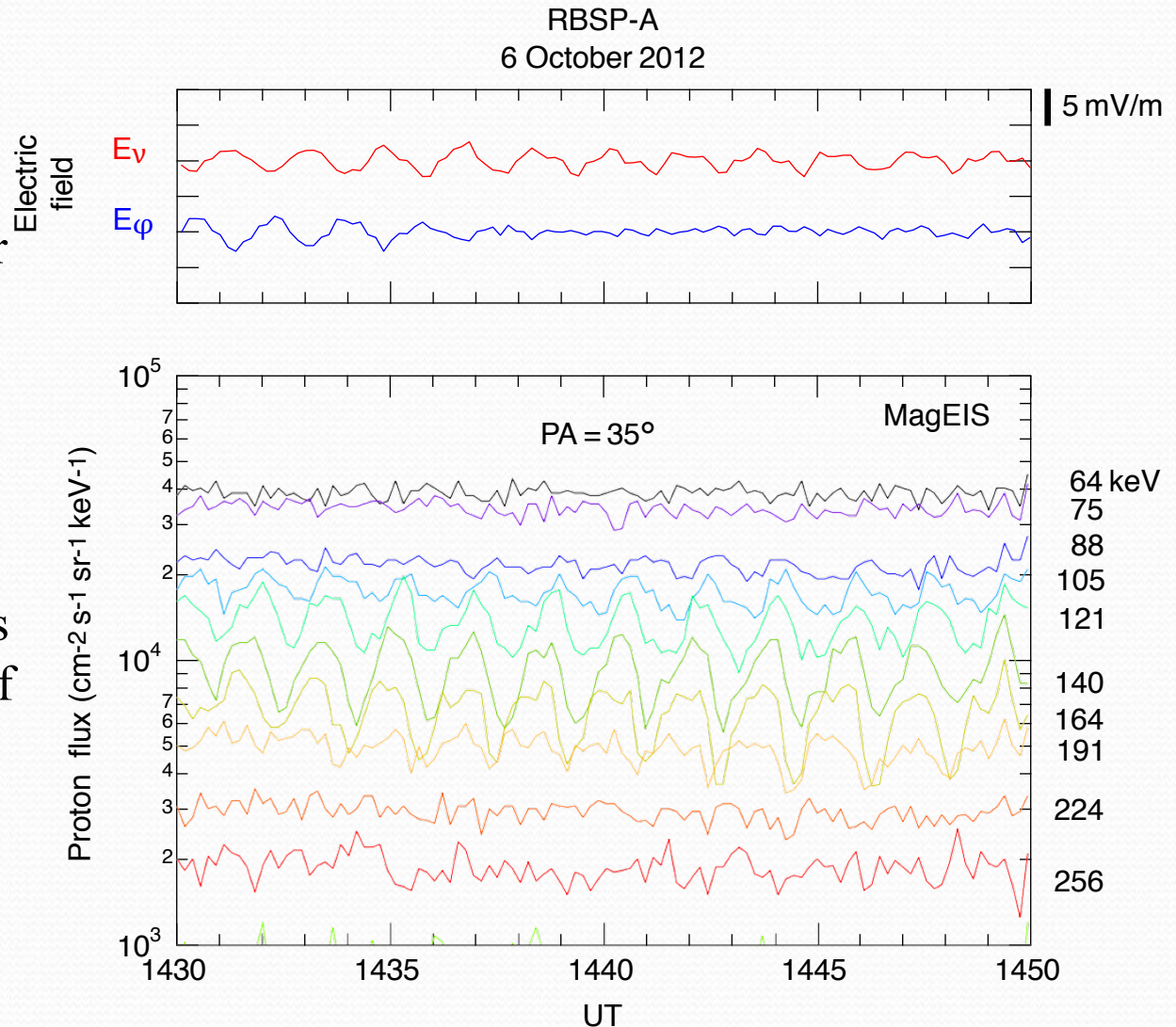


Takahashi, Fall  
AGU, 2016.

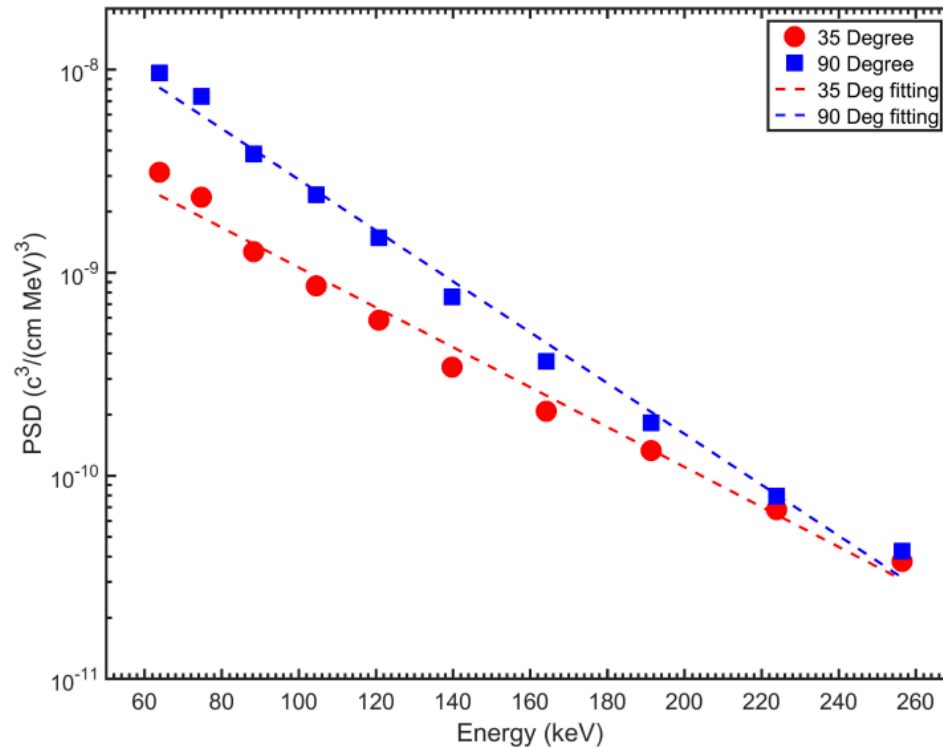


# RBSP-A Observations

- Modulations in the 35° PA flux peak near 150keV, the energy predicted by Southwood & Kivelson drift-resonance theory.
  - The flux at 90° shows almost no evidence of modulations.
- Takahashi, Fall AGU, 2016.

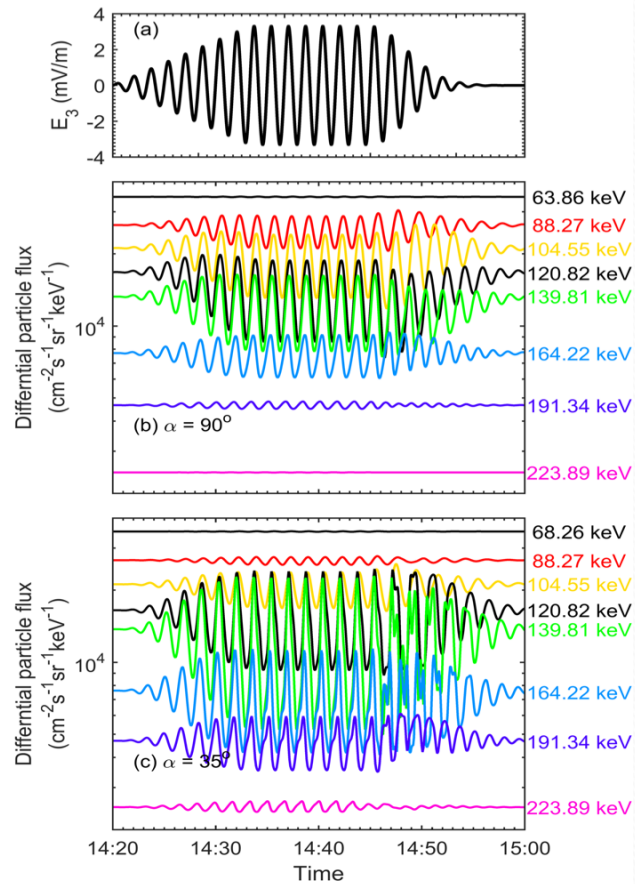
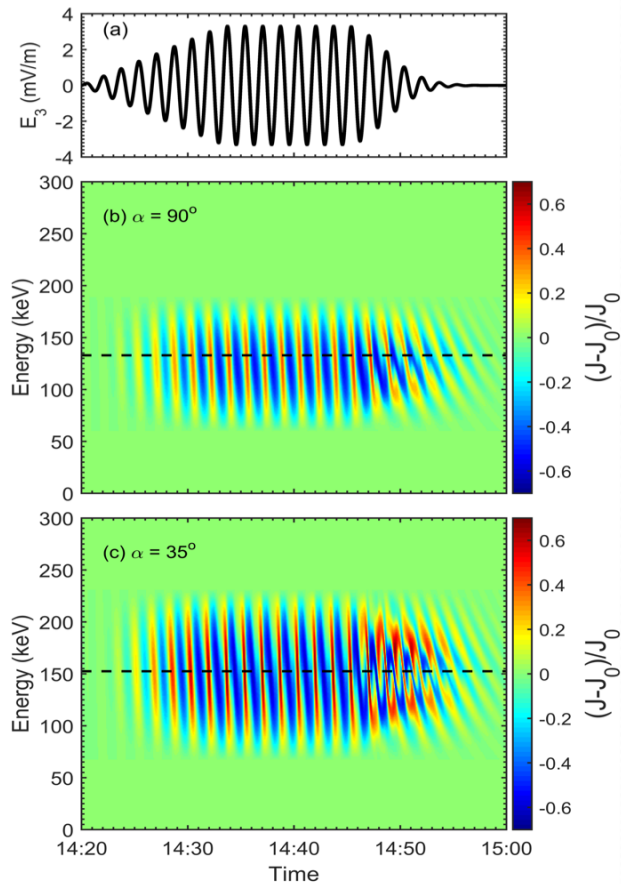


# RBSP-A Ion Temperature



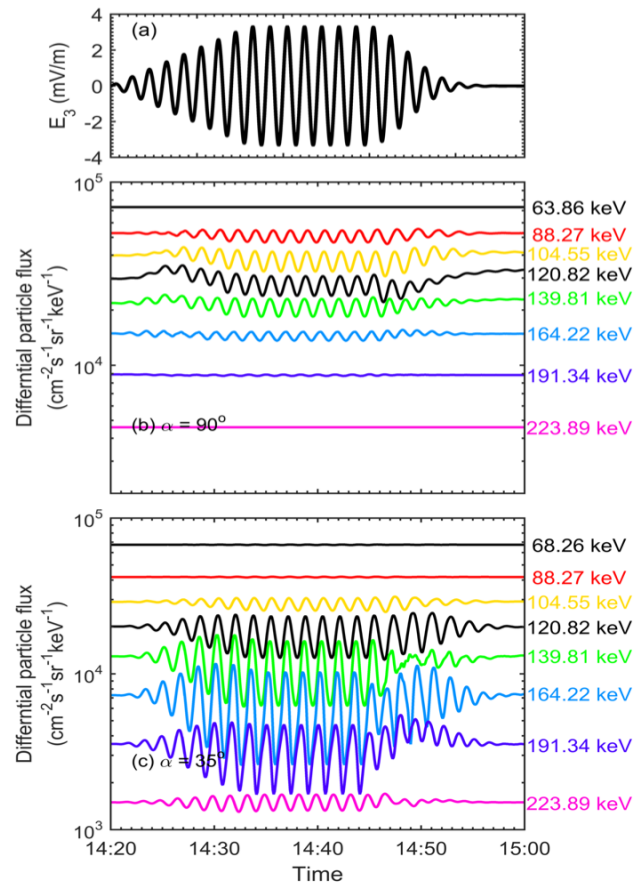
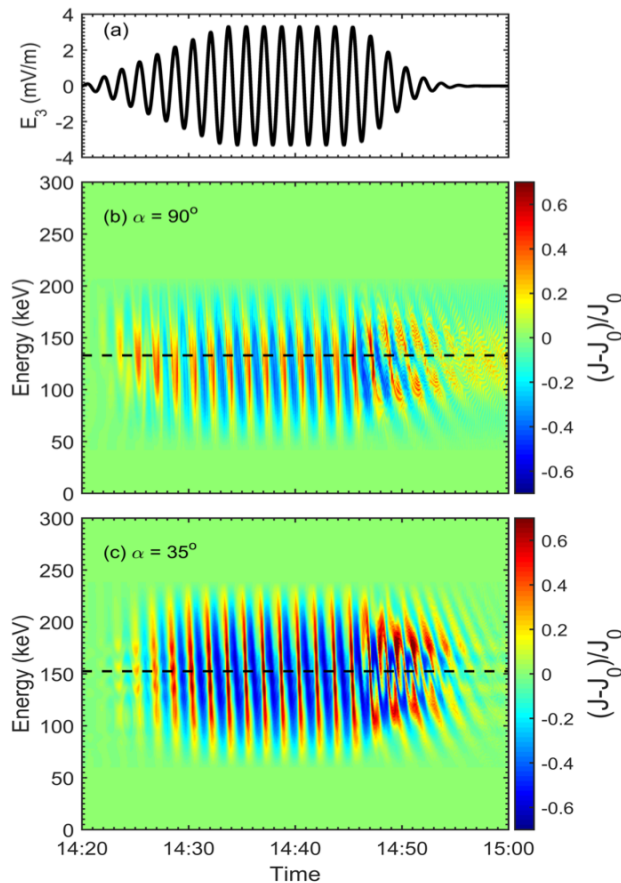
Time-averaged PSD from 14:30-14:50 UT. **Red circles and blue squares are MagEIS values at 35° and 90° PA, respectively.** Red and blue lines are obtained from linear regression. Estimated ambient ion temperature is between 35-41keV.

# PSD Reconstruction



RBSP-A measures significantly larger fluxes at  $35^\circ$  PA than at  $90^\circ$ . Model shows a much lesser reduction.

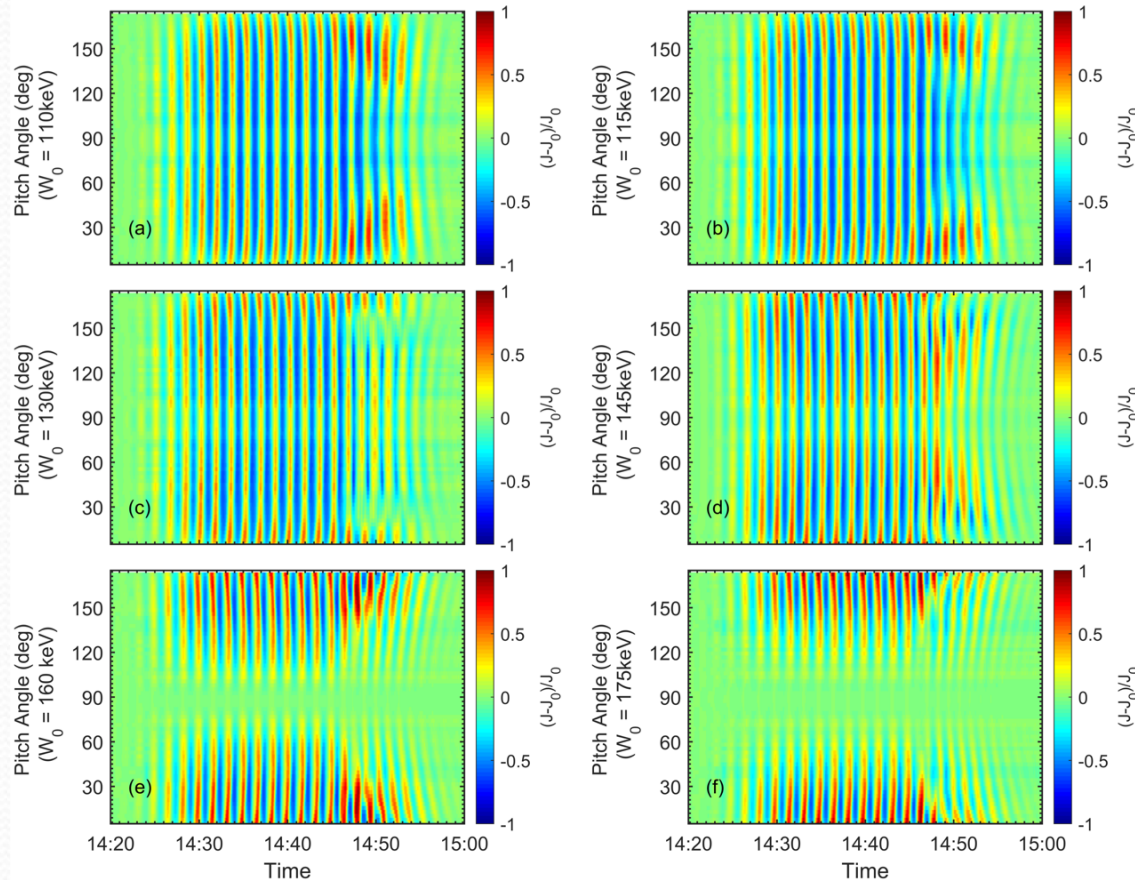
# PSD Reconstruction



A gradient is imposed on the initial PSD with an  $L^{-3}$  variation.

RBSP-A measures significantly larger fluxes at  $35^\circ$  PA than at  $90^\circ$ . The difference in flux in the model is now much closer to the spacecraft observations.

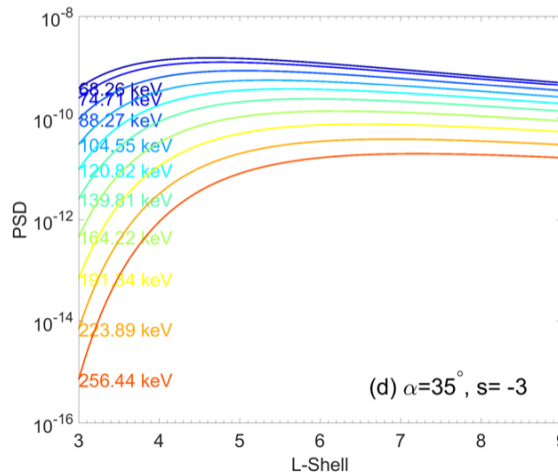
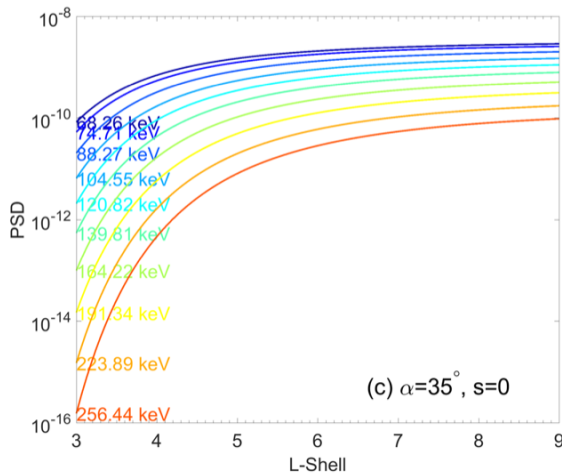
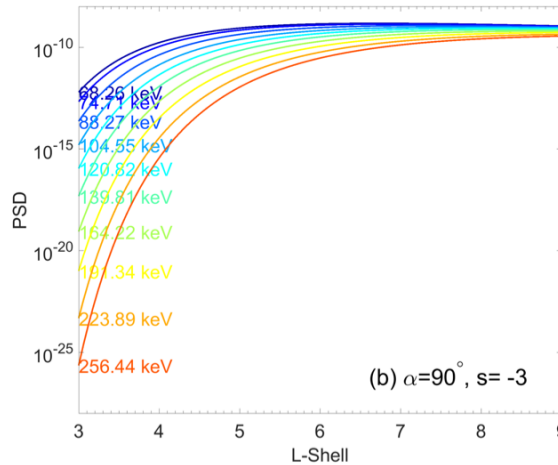
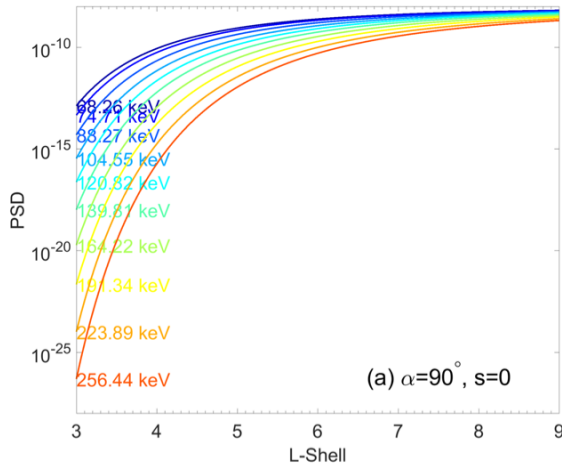
# Modeled PA Spectra



A gradient is imposed on the initial PSD with an  $L^{-3}$  variation.

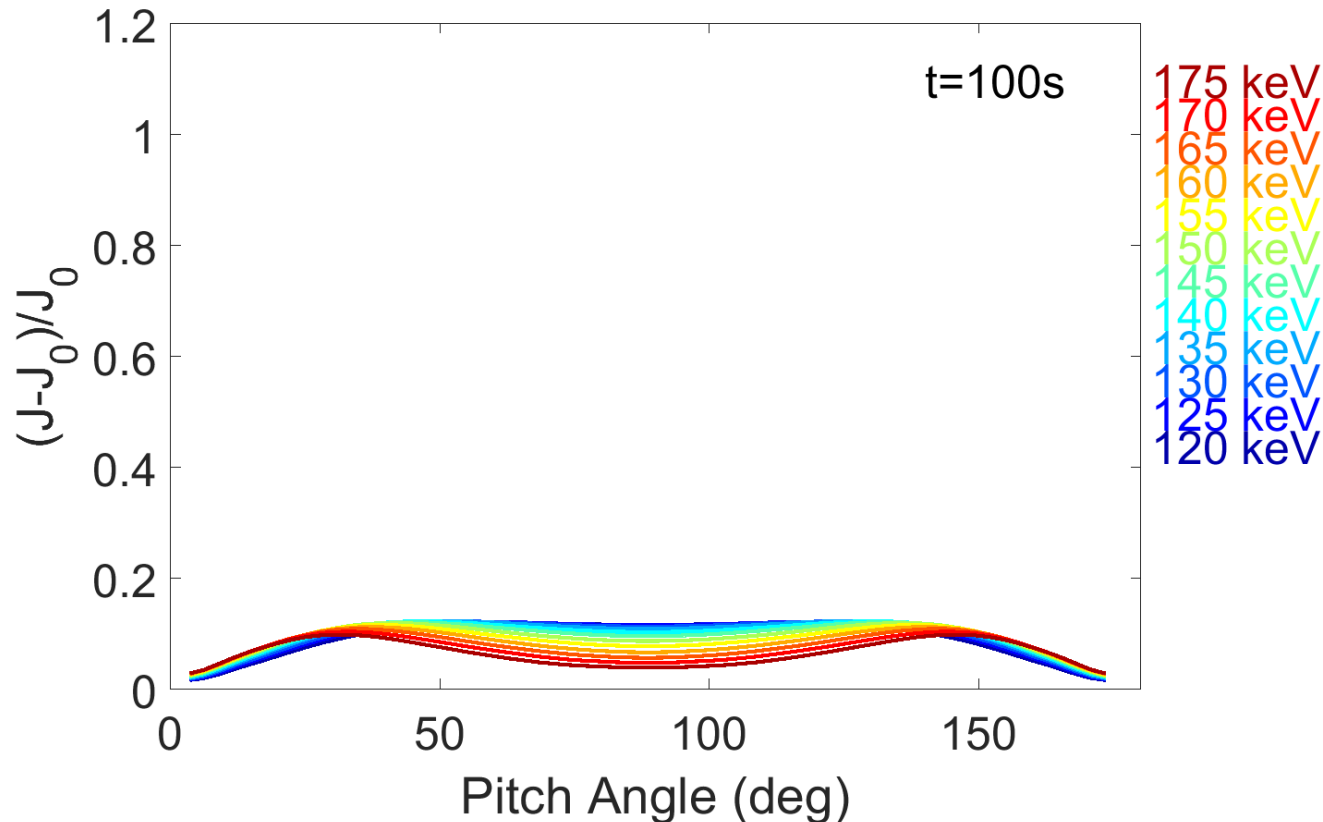
Energy changes of  $H^+$  as a function of PA and energy. The resonance energy is  $\sim 150\text{keV}$ . Absence of flux at  $90^\circ$  PA is consistent with VAPs.

# PSD Gradient Sensitivity



- **Left Column:** upward sloping outward gradient. No imposed L-dependence of PSD.
- **Right Column:** downward sloping gradient at the resonance location. A PSD varying as  $L^{-3}$  is assumed.
- **Right Column:**  $35^\circ$  PA ions have increased inward PSD gradient while  $90^\circ$  PSD flattens (no net acceleration).

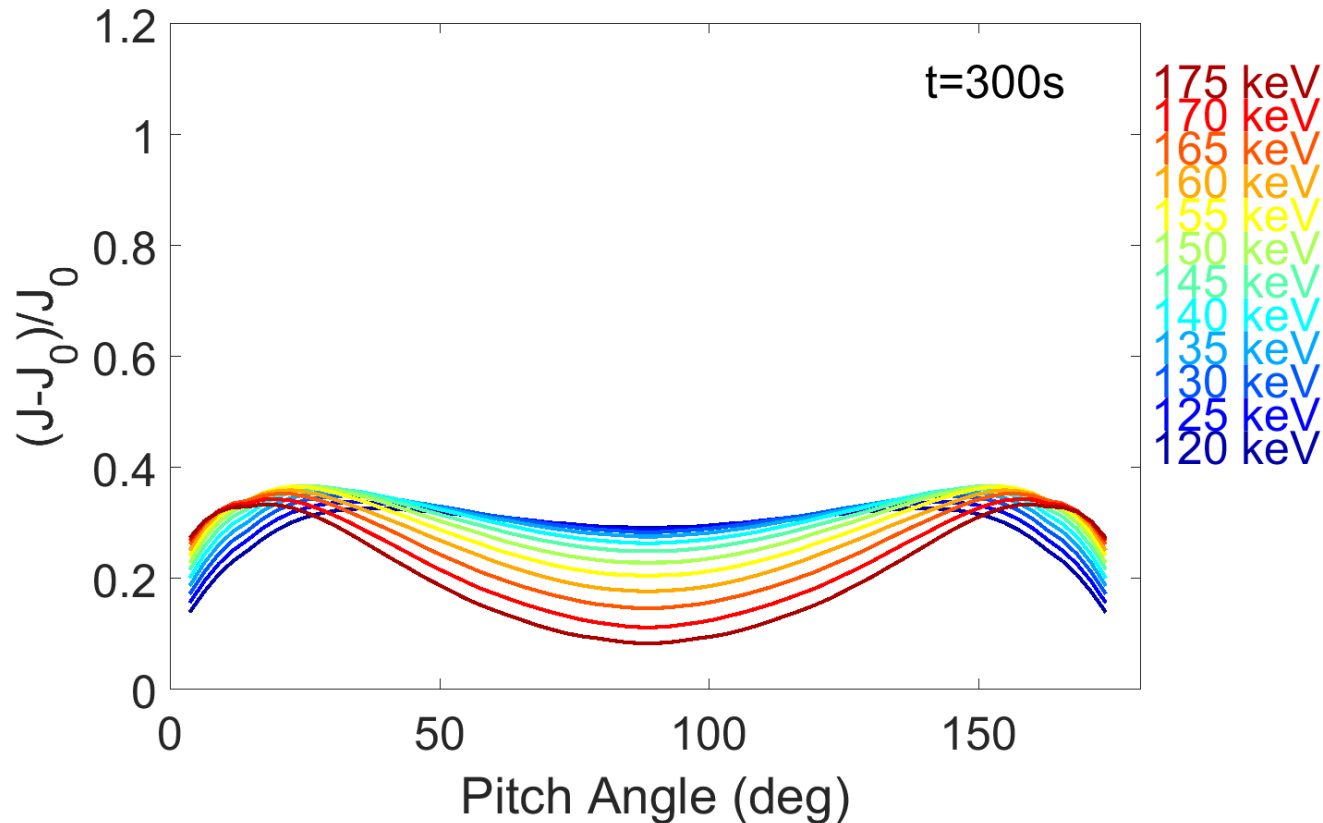
# Butterfly's



Energy changes of  $H^+$  ions as function of pitch angle for different energy bins. The 150keV energy channel is closer to the resonance energy. The pitch angle dependence of the resonance energy explains the behavior illustrated.

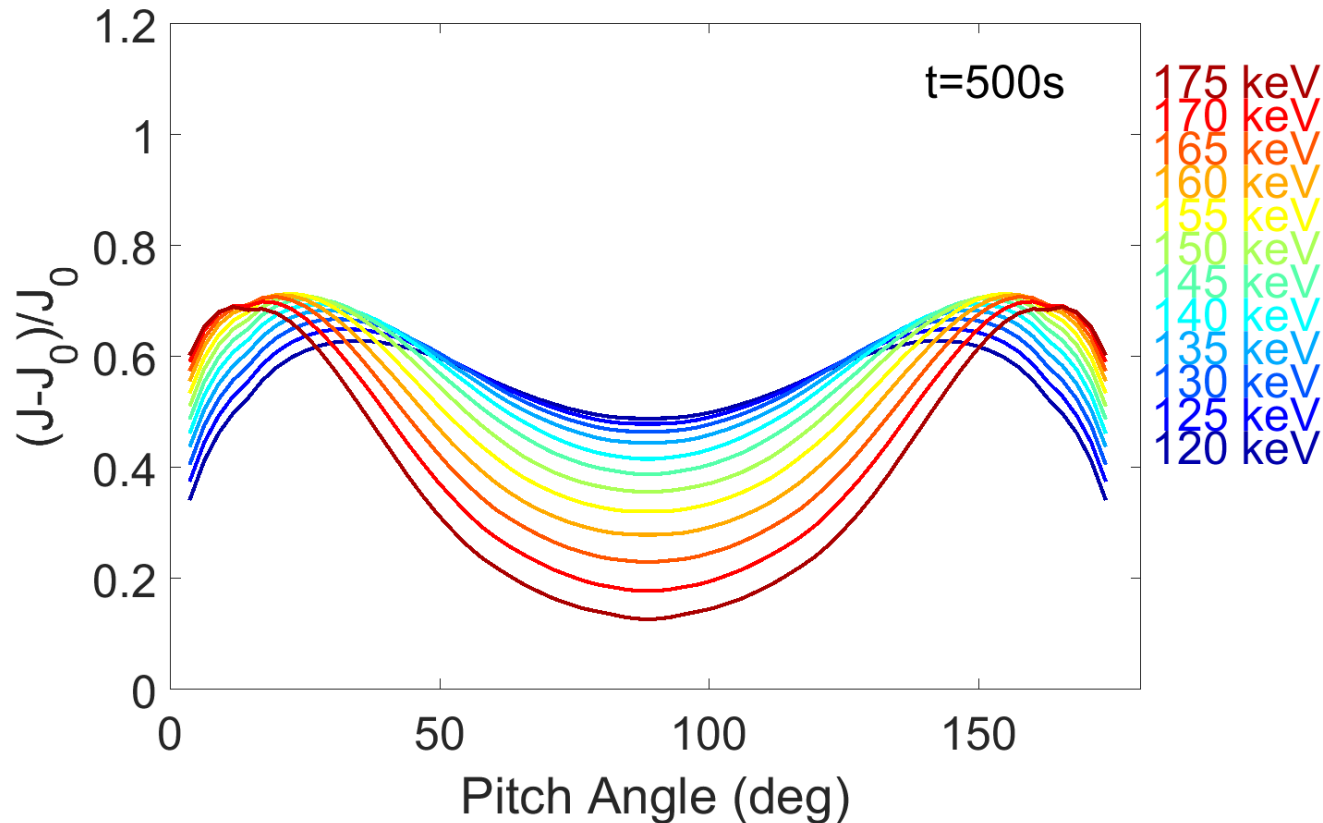


# Butterfly's



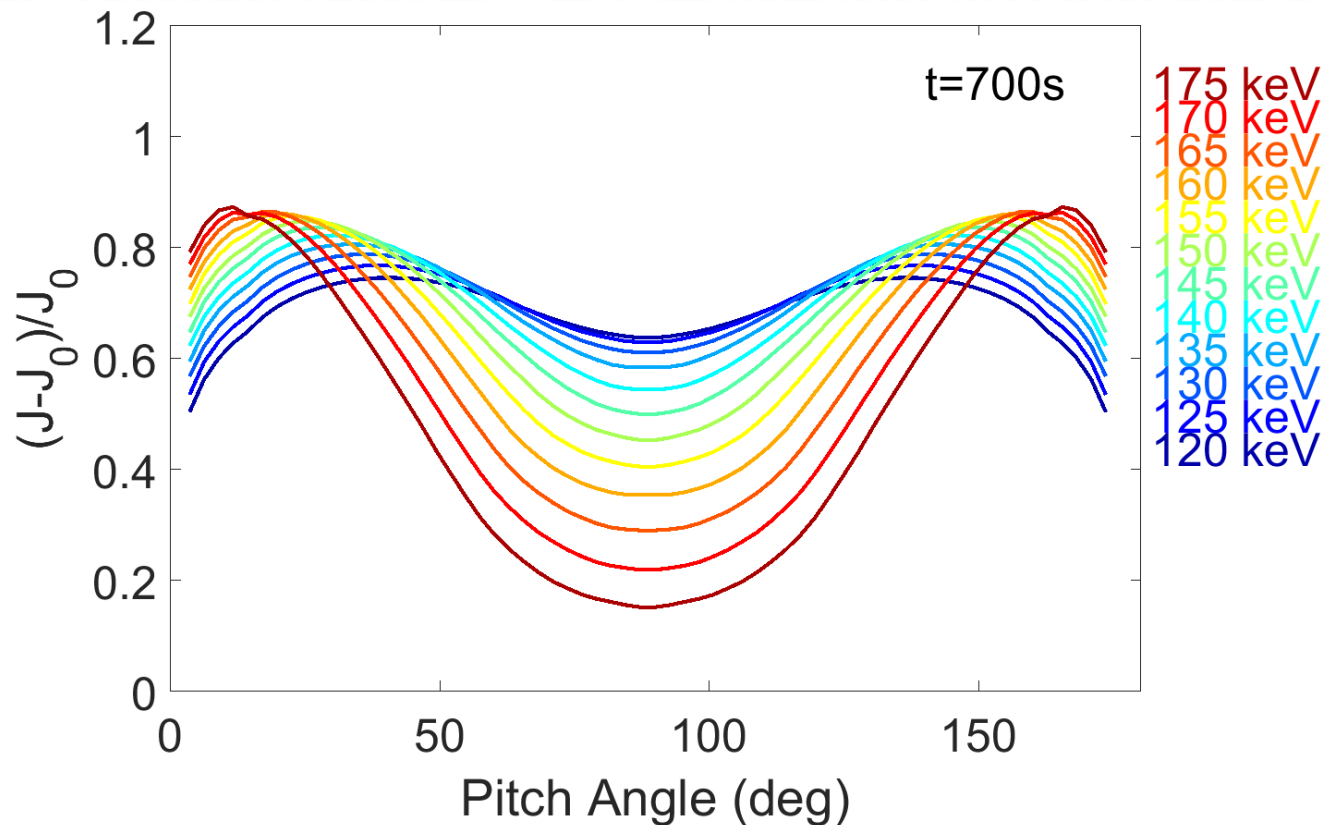
Energy changes of  $H^+$  ions as function of pitch angle for different energy bins. The 150keV energy channel is closer to the resonance energy. The pitch angle dependence of the resonance energy explains the behavior illustrated.

# Butterfly's



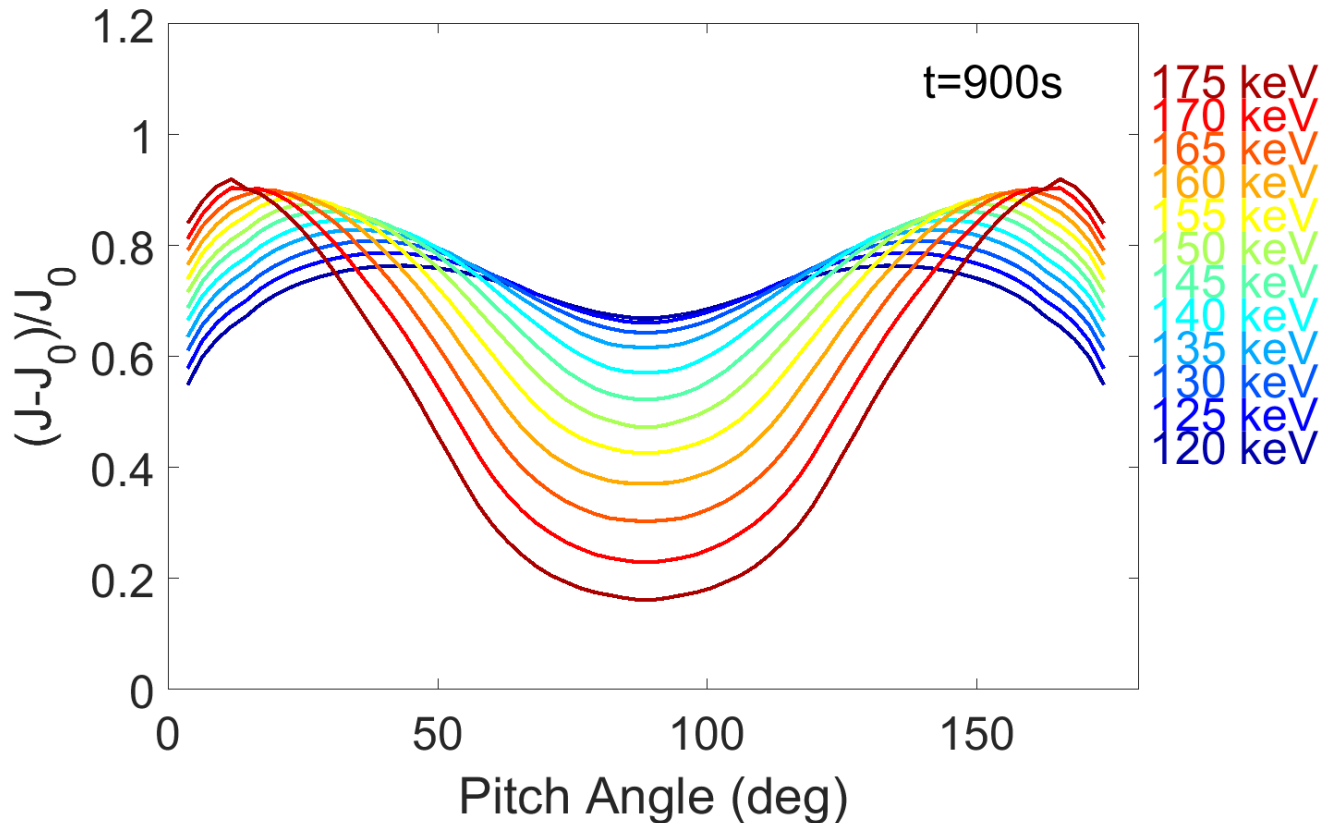
Energy changes of  $H^+$  ions as function of pitch angle for different energy bins. The 150keV energy channel is closer to the resonance energy. The pitch angle dependence of the resonance energy explains the behavior illustrated.

# Butterfly's



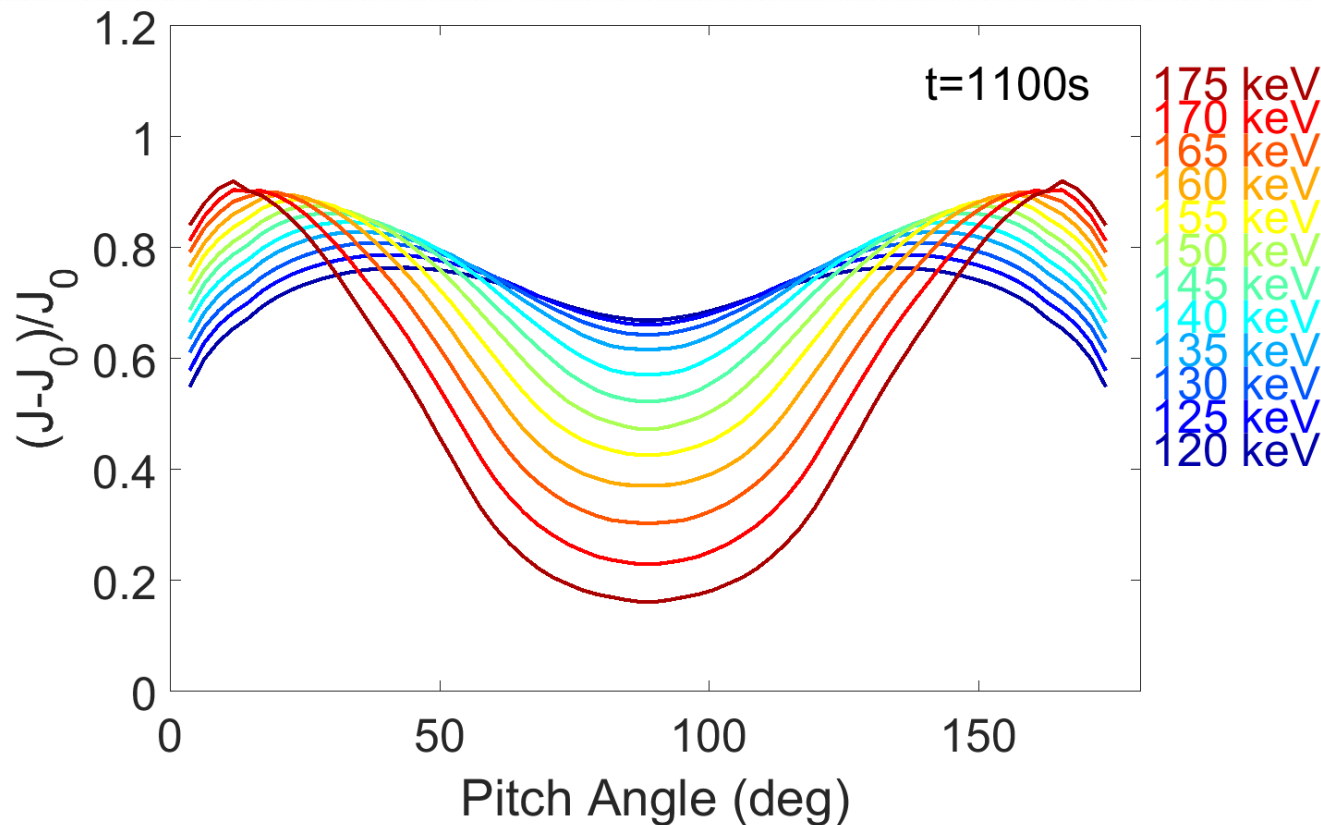
Energy changes of  $H^+$  ions as function of pitch angle for different energy bins. The 150keV energy channel is closer to the resonance energy. The pitch angle dependence of the resonance energy explains the behavior illustrated.

# Butterfly's



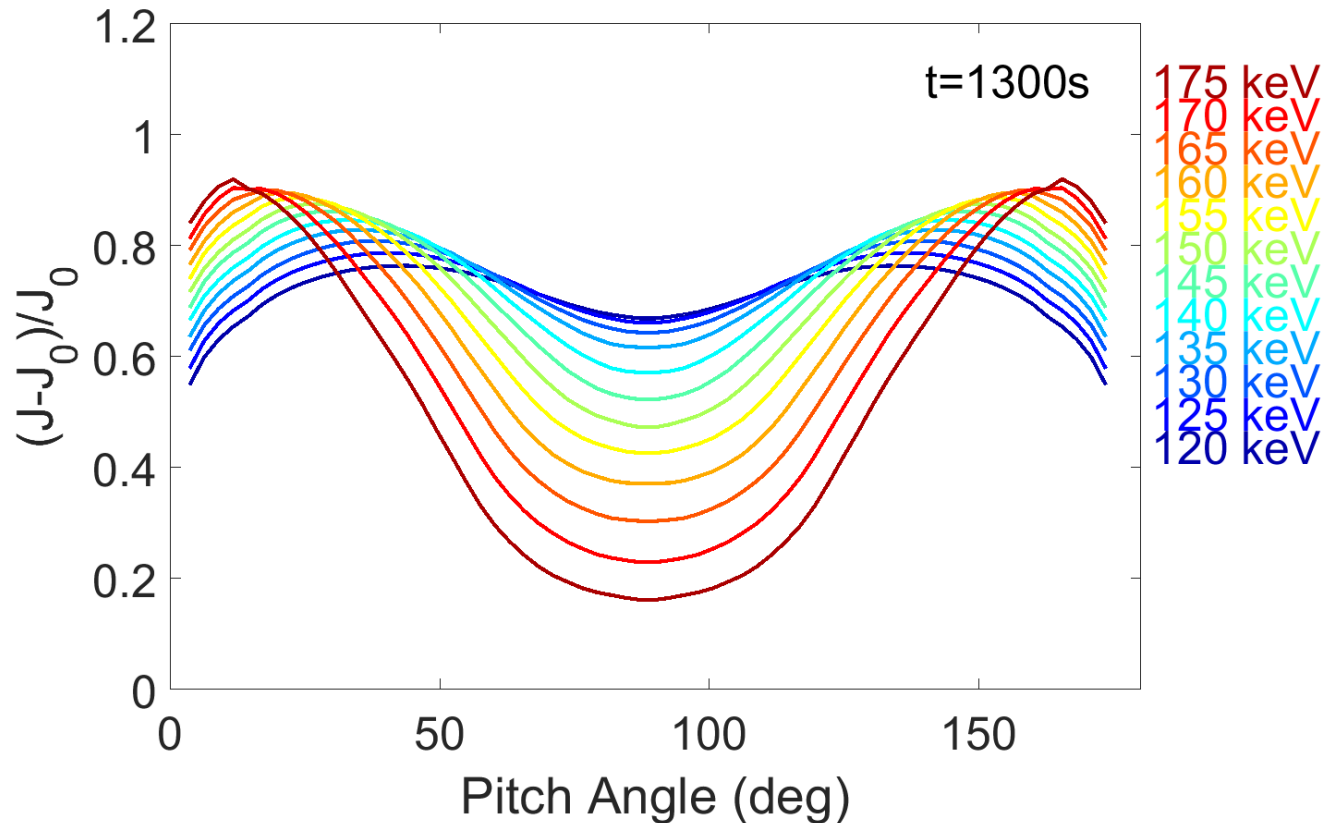
Energy changes of  $H^+$  ions as function of pitch angle for different energy bins. The 150keV energy channel is closer to the resonance energy. The pitch angle dependence of the resonance energy explains the behavior illustrated.

# Butterfly's



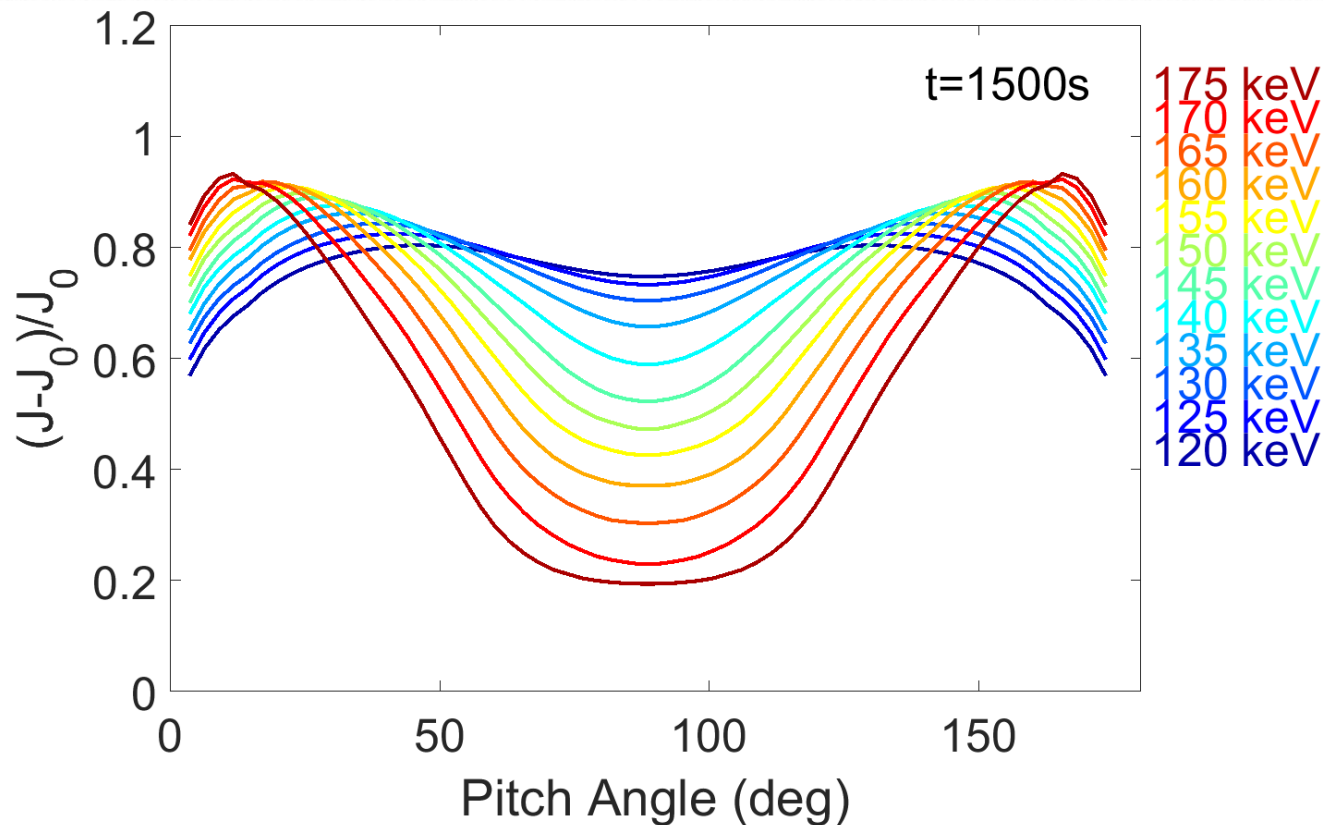
Energy changes of  $H^+$  ions as function of pitch angle for different energy bins. The 150keV energy channel is closer to the resonance energy. The pitch angle dependence of the resonance energy explains the behavior illustrated.

# Butterfly's



Energy changes of  $H^+$  ions as function of pitch angle for different energy bins. The 150keV energy channel is closer to the resonance energy. The pitch angle dependence of the resonance energy explains the behavior illustrated.

# Butterfly's



Energy changes of  $H^+$  ions as function of pitch angle for different energy bins. The 150keV energy channel is closer to the resonance energy. The pitch angle dependence of the resonance energy explains the behavior illustrated.

# Conclusions

- Test particle simulations using fields from a simple 3D model of ULF waves confirm predictions of Southwood-Kivelson theory.
- Resonant particles follow constant wave phase and move inward and outward over a range of  $L$  that depends on both the wave amplitude and radial extent in the EP.
- Remarkably, simplified models of ULF waves reproduce (quantitatively) energy and PA signatures of drift resonant electrons and ions observed by the Van Allen Probes [Claudepierre et al., GRL, 2013; Takahashi et al., JGR, 2018].
- Ions are particularly sensitive to gradients in PSD and naturally form butterfly-like distributions. Electrons undergoing drift-resonance do not.